



Silanes Hot Paper

How to cite: *Angew. Chem. Int. Ed.* **2020**, 59, 23132–23136

International Edition: doi.org/10.1002/anie.202011696

German Edition: doi.org/10.1002/ange.202011696

Isolable Silicon-Based Polycations with Lewis Superacidity

André Hermannsdorfer and Matthias Driess*

Dedicated to Professor Helmut Schwarz

Abstract: Molecular silicon polycations of the types R_2Si^{2+} and RSi^{3+} ($R = H$, organic groups) are elusive Lewis superacids and currently unknown in the condensed phase. Here, we report the synthesis of a series of isolable terpyridine-stabilized R_2Si^{2+} and RSi^{3+} complexes, $[R_2Si(terpy)]^{2+}$ ($R = Ph$ **1**²⁺; $R_2 = C_{12}H_8$ **2**²⁺, $(CH_2)_3$ **3**²⁺) and $[RSi(terpy)]^{3+}$ ($R = Ph$ **4**³⁺, cyclohexyl **5**³⁺, *m*-xylyl **6**³⁺), in form of their triflate salts. The stabilization of the latter is achieved through higher coordination and to the expense of reduced fluoride-ion affinities, but a significant level of Lewis superacidity is nonetheless retained as verified by theory and experiment. The complexes activate $C(sp^3)-F$ bonds, as showcased by stoichiometric fluoride abstraction from 1-fluoroadamantane (AdF) and the catalytic hydrodefluorination of AdF. The formation of the crystalline adducts $[2(F)]^+$ and $[5(H)]^+$ documents in particular the high reactivity towards fluoride and hydride donors.

Main group Lewis acids (LA) have garnered increasing attention over the last two decades with the emerging concept of frustrated Lewis pairs contributing significantly to this development.^[1–3] With the need for potent LAs, the focus often lies on Lewis superacids (LSA), that are defined as “molecular LAs, which are stronger than monomeric SbF_5 in the gas phase”, according to Krossing.^[4] Recent reports on Lewis superacidic perhalogenated bis(catecholato)germanes^[5] and -silanes^[6] emphasize the great potential of molecular main group LAs, with silicon-based LAs being particularly attractive due to the high abundance and low toxicity of this element. Furthermore, silylium ions, R_3Si^+ , are well-established as valuable catalysts in organic synthesis^[7,8] and exhibit high fluoride ion affinities (FIAs), which categorize them as LSAs.^[3,9] Expectedly, molecular silicon(IV) dications of the type R_2Si^{2+} represent stronger LAs (e.g., $FIA(SiF_2^{2+}) = 2167 \text{ kJ mol}^{-1}$),^[10] but such species are

unknown in the condensed phase; merely SiH_2^{2+} and SiF_2^{2+} were observed in mass spectrometry.^[11] To date, there is no experimental evidence for the formation of RSi^{3+} and repulsive.^[12] Further stabilization is required in order to make such gas-phase molecules accessible in the condensed phase. In this regard, the formation of complexes with neutral Lewis bases represents a viable approach towards isolable silicon-based polycations (cf. Figure 1). However, increased stability comes at the cost of lower electrophilicity and Lewis acidity. Accordingly, numerous di- and tetracationic silicon complexes with hexacoordinated Si^{IV} atoms are even water stable.^[13]

Here, we demonstrate that silicon-based polycations retain Lewis superacidic features upon stabilization with the terpyridine ligand (terpy) and in the presence of the OTf (CF_3SO_3 ; triflate) counter anion. Their Lewis superacidity is confirmed theoretically ($FIA > SbF_5$) and experimentally (F^- abstraction from SbF_6^-). Further reactivity investigations revealed that they are one of the strongest silicon-based LAs known to date. The Lewis acidity of dications R_2Si^{2+} and their terpy complexes $[R_2Si(terpy)]^{2+}$ was assessed by determining isodesmic FIAs using the TMS-reference system^[14] (Table 1, for computational details see *Supporting Information*). Expectedly, dicationic R_2Si^{2+} ($FIA > 1450 \text{ kJ mol}^{-1}$) are stronger LAs than R_3Si^+ ($700–950 \text{ kJ mol}^{-1}$).^[3,15] Notably, through terpy-coordination, the FIAs of $[R_2Si(terpy)]^{2+}$ are about 35–40% lower than those of “free” R_2Si^{2+} , but still well above the SbF_5 threshold of 500 kJ mol^{-1} . An estimation of solvation correction in CH_2Cl_2 was included (FIA_{solv}) using the C-PCM solvation model,^[16] as gas phase FIAs of cations often contain strong contributions of charge neutralization and electrostatic attraction.^[3,17] This resulted in a pronounced FIA-damping for R_2Si^{2+} and $[R_2Si(terpy)]^{2+}$. The reduced

[*] M. Sc. A. Hermannsdorfer, Prof. Dr. M. Driess
Department of Chemistry: Metalorganics and Inorganic Materials,
Technische Universität Berlin
Strasse des 17. Juni 115, Sekr. C2, 10623 Berlin (Germany)
E-mail: matthias.driess@tu-berlin.de

Supporting information and the ORCID identification number(s) for the author(s) of this article can be found under:
<https://doi.org/10.1002/anie.202011696>.

© 2020 The Authors. Published by Wiley-VCH GmbH. This is an open access article under the terms of the Creative Commons Attribution Non-Commercial NoDerivs License, which permits use and distribution in any medium, provided the original work is properly cited, the use is non-commercial and no modifications or adaptations are made.

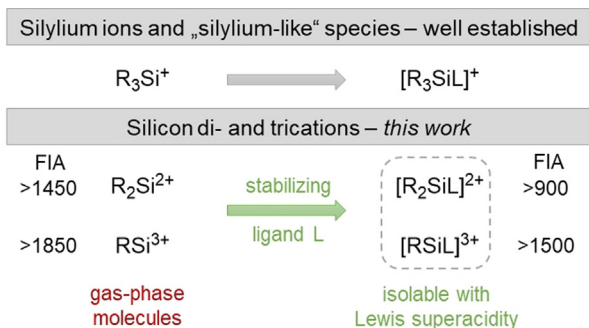


Figure 1. Previously studied silicon-based monocations and polycations (L = terpyridine; this work) with their fluoride ion affinities (FIA [kJ mol^{-1}]).

Table 1: DFT-derived fluoride ion affinities (FIA) and solvent corrected FIAs (FIA_{solv}) of the cations R_2Si^{2+} and their terpyridine complexes in kJ mol^{-1} .

	$\text{Ph}_2\text{Si}^{2+}$	$\mathbf{1}^{2+}$	$(\text{C}_{12}\text{H}_8)\text{Si}^{2+}$	$\mathbf{2}^{2+}$	$(\text{CH}_2)_3\text{Si}^{2+}$	$\mathbf{3}^{2+}$
FIA^{a}	1459	934	1541	982	1622	1000
$FIA_{\text{solv}}^{\text{b}}$	673	263	767	306	691	296

[a] B3LYP-D3B]/def2svp//PW6B95-D3B]/def2qzvpp [b] B3LYP-D3B]/def2svp, gas phase geometries with C-PCM solvation model in CH_2Cl_2 .

positive charge around the Si centers in the terpy-ligated $R_2\text{Si}^{2+}$ moieties can be visualized by mapping of the electrostatic potential on a $0.025 e^- \text{Bohr}^{-3}$ isodensity surface (Figure 2). Areas with blue color-coding represent sections which are more positively charged, whereas the delocalization of the positive charges in $[\text{R}_2\text{Si}(\text{terpy})]^{2+}$ results in areas with lower potential (red color-coding = less positively charged), notably also around the Si centers.

In contrast to the reported synthesis of the $[\text{Ph}(\text{terpy})]^{2+}$ phosphorus dication from PhPCl_2 ,^[18] attempts to obtain analogous cations directly from dichlorosilanes failed. However, treatment of the corresponding $R_2\text{Si}(\text{OTf})_2$ ditriflates ($R_2 = \text{Ph}_2, (\text{CH}_2)_3, \text{C}_{12}\text{H}_8$) with terpy afforded the stable complex salts $\mathbf{1}[\text{OTf}]_2$, $\mathbf{2}[\text{OTf}]_2$ and $\mathbf{3}[\text{OTf}]_2$ in 73–93% yields (Scheme 1), which were fully characterized by NMR, IR, CHN analysis and SC-XRD. The Si centers are penta- ($\mathbf{1}^{2+}$) or hexacoordinated ($\mathbf{2}^{2+}$ and $\mathbf{3}^{2+}$) in the solid state (Figure 3), but ^1H , ^{13}C and ^{19}F NMR spectra imply that the Si-OTf interactions are labile in solutions.

The Lewis superacidity of $\mathbf{1}[\text{OTf}]_2$, $\mathbf{2}[\text{OTf}]_2$, and $\mathbf{3}[\text{OTf}]_2$ was confirmed by reactions with $[\text{PPh}_4][\text{SbF}_6]$ in CD_3CN . In all cases, fluoride abstraction from SbF_6^- leads to the formation of “SiF” species as observed by ^{19}F NMR

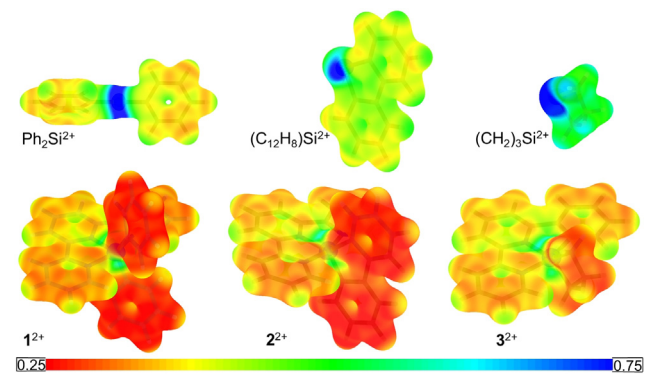


Figure 2. Projection of the calculated electrostatic potential (B3LYP-D3B]/def2svp) onto the isodensity surface ($0.025 e^- \text{Bohr}^{-3}$) of the dications $R_2\text{Si}^{2+}$ (top) and their terpyridine complexes $[\text{R}_2\text{Si}(\text{terpy})]^{2+}$ (bottom).



Scheme 1. Synthesis of the triflate salts of the dications $\mathbf{1}^{2+}$, $\mathbf{2}^{2+}$ and $\mathbf{3}^{2+}$.

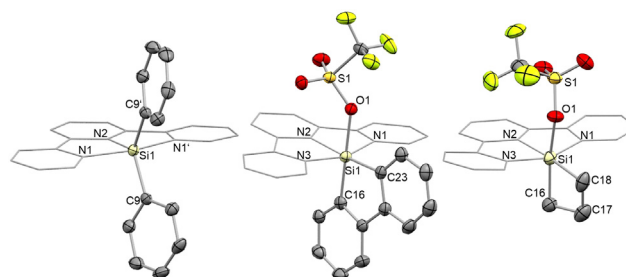


Figure 3. Molecular structures of $\mathbf{1}^{2+}$, $[\mathbf{2}(\text{OTf})]^+$ and $[\mathbf{3}(\text{OTf})]^+$ (from left to right; thermal ellipsoids at 50% probability; H atoms omitted for clarity and terpy ligand reduced to wireframe).

(Figure 4). For $\mathbf{1}^{2+}$, the formation of Ph_2SiF_2 ($\delta^{19}\text{F} -142.9$ ppm, $^1J_{\text{SiF}} = 291$ Hz)^[19] was observed after 20 h, while the product mixtures resulting from $\mathbf{2}^{2+}$ and $\mathbf{3}^{2+}$ could not be identified unambiguously. In order to avoid ligand scrambling and other side-reactions, the compounds were exposed to 1-fluoroadamantane (AdF) as a F^- source. Furthermore, $\text{C}(\text{sp}^3)\text{-F}$ bond activation is a crucial step for catalytic hydrodefluorination reactions (HDF) and silylium ions readily abstract F^- from fluorocarbons.^[2,7,20] ^{19}F NMR spectra of the reactions of $\mathbf{1}^{2+}$, $\mathbf{2}^{2+}$ and $\mathbf{3}^{2+}$ with AdF showed complete consumption of AdF in less than 1 h. With $\mathbf{1}^{2+}$, the generation of Ph_2SiF_2 was observed similarly to the results obtained with SbF_6^- . For $\mathbf{2}^{2+}$, SiF HMOC measurements showed the clean formation of $[\mathbf{2}(\text{F})]^+$ ($\delta^{29}\text{Si} -135.9$ ppm, $\delta^{19}\text{F} -112.5$ ppm, $^1J_{\text{SiF}} = 224$ Hz), which was isolated in 42% yield. SC-XRD analysis revealed a hexacoordinate Si center with a Si-F bond length of $1.6693(14)$ Å (Figure 4). The same species was detected in the reaction mixture of $\mathbf{2}[\text{OTf}]_2$ and $[\text{PPh}_4][\text{SbF}_6]$. Exposure of $\mathbf{3}[\text{OTf}]_2$ to AdF gave a complex mixture of products. Most likely, the strained silacyclobutane fragment is not stable under the reaction conditions. In fact, a ring-cleavage reaction was observed for the reaction of 1,1-difluorosilacyclobutane with KF .^[21]

Compared to $R_2\text{Si}^{2+}$, the determined FIAs for RSi^{3+} suggest a tremendous increase in Lewis acidity and reach almost 2000 kJ mol^{-1} (cf. Table 2). The transition to the four-coordinate $[\text{RSi}(\text{terpy})]^{3+}$ results in FIAs decreased by only ca. 20% ($> 1500 \text{ kJ mol}^{-1}$), which lie above the FIA of the two-coordinate borenium cation $[(\text{catecholato})\text{B}]^+$ (1210 kJ mol^{-1}).^[3,22] Solvation damping is pronounced for the triply charged species but the obtained FIA_{solv} for $\mathbf{4}^{3+}$, $\mathbf{5}^{3+}$

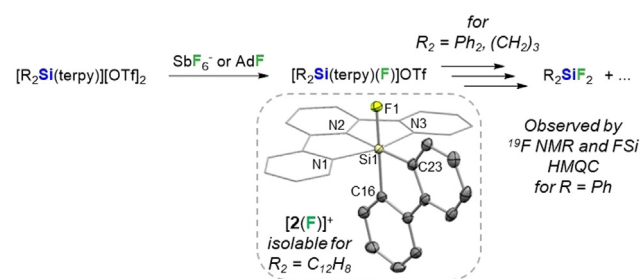


Figure 4. Reaction of $[\text{R}_2\text{Si}(\text{terpy})][\text{OTf}]_2$ with $[\text{PPh}_4][\text{SbF}_6]$ or 1-fluoroadamantane (AdF) and the molecular structure of $[\mathbf{2}(\text{F})]^+$ (thermal ellipsoids at 50% probability; Si-F $1.6693(14)$ Å).

Table 2: DFT-derived fluoride ion affinities (FIA) and solvent corrected FIAs (FIA_{solv}) of cations RSi^{3+} and their terpyridine complexes in kJ mol^{-1} .

	$PhSi^{3+}$	4^{3+}	$CySi^{3+}$	5^{3+}	$m\text{-XylSi}^{3+}$	6^{3+}
FIA^{a}	1951	1522	— ^[c]	1542	1890	1519
$FIA_{\text{solv}}^{\text{b}}$	764	563	—	566	767	564

[a] B3LYP-D3BJ/def2svp//PW6B95-D3BJ/def2qzvpp [b] B3LYP-D3BJ/def2svp, gas phase geometries with C-PCM solvation model in CH_2Cl_2 . [c] No global minimum was found for $CySi^{3+}$.

and 6^{3+} surpass the FIA_{solv} of SbF_5 by more than 200 kJ mol^{-1} . Electrostatic potential maps illustrate the “smearing” of the positive charge over the larger complex cations when comparing RSi^{3+} and $[RSi(\text{terpy})]^{3+}$ (Figure 5). However, regions with high potential remain around the silicon centers also for $[RSi(\text{terpy})]^{3+}$ (blue color-coding), which is in agreement with the high FIAs despite the additional coordination.

The stable $4[\text{OTf}]_3$, $5[\text{OTf}]_3$ and $6[\text{OTf}]_3$ triflate salts were obtained in 83–91% yields from $RSi(\text{OTf})_3$ precursors (Scheme 2) with no sign of decomposition upon storage over >6 months under inert atmosphere. X-Ray structure analyses of $4[\text{OTf}]_3$ and $6[\text{OTf}]_3$ indicate that the anions provide further stabilization through interaction with the silicon centers (Figure 6A). NMR data show the dynamic exchange of coordinating and “free” triflate anions for $5[\text{OTf}]_3$ and $6[\text{OTf}]_3$ in solutions, whereas two singlets are observable for Si-OTf and OTf^- in the ^{19}F NMR spectrum of $4[\text{OTf}]_3$ in CD_2Cl_2 .

The Lewis superacidity of $4[\text{OTf}]_3$, $5[\text{OTf}]_3$ and $6[\text{OTf}]_3$ was confirmed experimentally by fluoride abstraction from SbF_6^- . ^1H NMR measurements showed the consumption of the starting material promptly after mixing the respective complex salt with $[\text{PPh}_4][\text{SbF}_6]$ in CD_3CN . Furthermore, ^{19}F and FSi-HMQC NMR measurements gave evidence for the

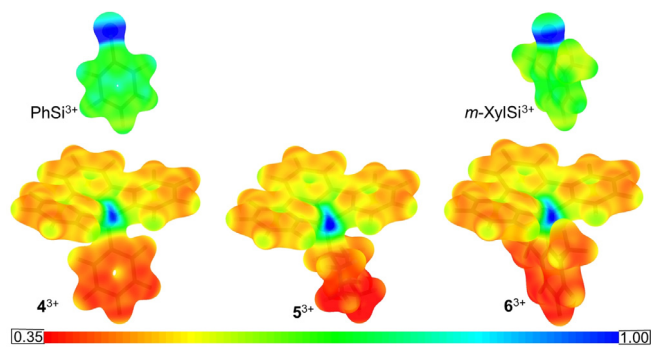


Figure 5. Projection of the calculated electrostatic potential (B3LYP-D3BJ/def2svp) onto the isodensity surface ($0.025 e^- \text{ Bohr}^{-3}$) of trications RSi^{3+} (top) and their terpy complexes $[RSi(\text{terpy})]^{3+}$ (bottom). No minimum geometry was found for $CySi^{3+}$.



Scheme 2. Synthesis of the triflate salts of trications 4^{3+} , 5^{3+} and 6^{3+} .

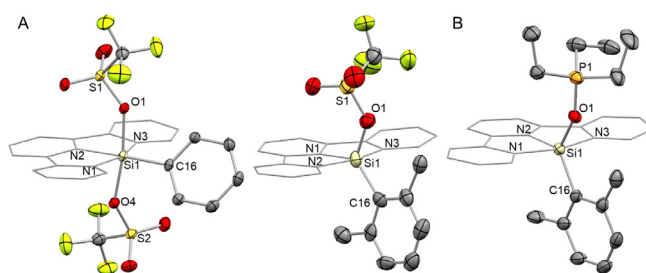


Figure 6. Molecular structures of $[4(\text{OTf})_2]^{2+}$, $[6(\text{OTf})]^{2+}$ (A) and $[6(\text{OPEt}_3)]^{3+}$ (B) (from left to right; thermal ellipsoids at 50% probability; H atoms are omitted for clarity and terpy ligand reduced to wireframe).

formation of several species with a SiF bond. F^- abstraction from AdF gave cleaner reactions with two unidentified major products from $4[\text{OTf}]_3$ and $6[\text{OTf}]_3$, respectively, and a single product from $5[\text{OTf}]_3$ (probably $[5(\text{F})][\text{OTf}]_2$, see *Supporting Information*). The corresponding SiF species were also observed in the respective reactions with $[\text{PPh}_4][\text{SbF}_6]$.

Further Lewis acidity scaling with the Gutmann-Beckett (GB) method, that relies on the induced ^{31}P NMR shift $\Delta^{31}\text{P}$ of OPEt_3 upon coordination to a LA,^[23] gave the lowest $\Delta^{31}\text{P}$ for $1^{2+}\cdot\text{OPEt}_3$ (23.5 ppm, cf. Figure S26). This is in agreement with the lower FIA compared to the strained silacyclobutane and silafluorene derivatives 2^{2+} and 3^{2+} ($\Delta^{31}\text{P} = 28.6, 27.7$ ppm), which exceed the reported $\Delta^{31}\text{P}$ for $\text{B}(\text{C}_6\text{F}_5)_3\cdot\text{OPEt}_3$ in CH_2Cl_2 (26 ppm).^[24] X-Ray structure analyses confirmed the formation of octahedral $[2(\text{OPEt}_3)]^{2+}$ and $[3(\text{OPEt}_3)]^{2+}$ (Figures S101 and S102). With $4[\text{OTf}]_3$ and $5[\text{OTf}]_3$, mixtures of bis-adducts and other unidentified species formed ($\Delta^{31}\text{P}$ ranging from 35.5 to 48.9 ppm), which hampered a meaningful scaling with the GB method (see *Supporting Information*). Remarkably, the well-defined mono-adduct $[6(\text{OPEt}_3)]^{3+}$ formed from an equimolar mixture of $6[\text{OTf}]_3$ and OPEt_3 . NMR spectroscopy ($\delta^{29}\text{Si} -92.0$ ppm) and SC-XRD (Figure 6B) confirmed the presence of a pentacoordinate Si center. Strikingly, the resulting $\Delta^{31}\text{P}$ (61.1 ppm) for $[6(\text{OPEt}_3)]^{3+}$ not only exceeds the $\Delta^{31}\text{P}$ for OPEt_3 adducts of silylium ions (43.9 ± 2.7 ppm for $[\text{R}_3\text{Si}(\text{OPEt}_3)]^+$ ($\text{R} = \text{alkyl or aryl}$)^[9,22,25] but also for the borenium adduct $[(\text{catecholato})\text{B}(\text{OPEt}_3)]^+$ (60.7 ppm).^[9,22] While comparisons between different classes of compounds have to be considered with caution due to the large impact of steric and HSAB effects,^[26] the GB scaling nevertheless substantiates the ranking of 6^{3+} among the strongest silicon LAs known to date.

As a matter of fact, $5[\text{OTf}]_3$ and $6[\text{OTf}]_3$ react with triethylsilane (Et_3SiH) under hydride abstraction (Figure 7). Conclusively, HSi-HMQC NMR measurements showed the formation of Et_3SiOTf ($\delta^{29}\text{Si}$ 46–47 ppm)^[27] in both cases. The conversion to $[5(\text{H})][\text{OTf}]_2$ proceeded slowly at room temperature and was confirmed by independent synthesis from $\text{CySi}(\text{H})(\text{OTf})_2$ and terpy. SC-XRD analysis confirmed the connectivity of the pentacoordinate dication. Contrastingly, compound $6[\text{OTf}]_3$ was consumed within hours in presence of Et_3SiH with clear NMR spectroscopic evidence for the activation of the *para*-carbon of the terpy ligand (Figure 7,

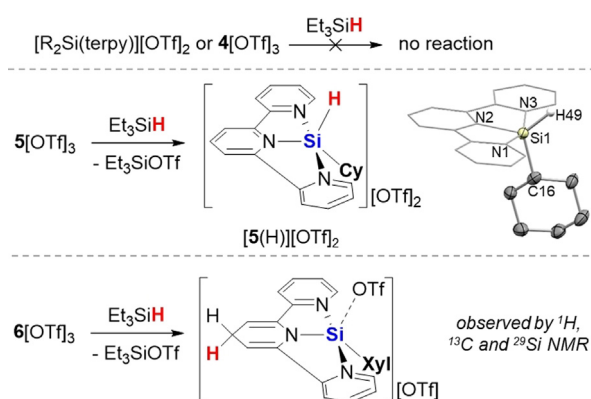


Figure 7. Reactivity of **5**[OTf]₃ and **6**[OTf]₃ towards Et₃SiH with depiction of the molecular structure of **[5(H)]**²⁺.

$\delta^{29}\text{Si}$ –94.8 ppm, see *Supporting Information*). Recently, a similar carbon-centered Lewis acidity was reported for a series of *N*-heterocycle-ligated borocations^[28] and for terpy-stabilized P^V dications.^[29] Furthermore, the catalytic cycle for the hydrosilylation of pyridines to 1-silyl-4-hydropyridines is supposed to involve hydride transfer to *N*-silyl-pyridinium cations.^[30] We attribute the activation of the terpy-backbone to the lower spatial accessibility of the silicon center in **6**³⁺.

Finally, the applicability of the silicon cations in the catalytic HDF of AdF with Et₃SiH was demonstrated with a catalyst loading of 10 mol % (Table 3). The low respective yields of Et₃SiF may be attributed to the formation of stable fluoride adducts and fluorosilanes (vide supra). The catalytic efficiencies correlate well to the scaled Lewis acidities (**1**²⁺ < **2**²⁺, **3**²⁺ < **4**³⁺, **5**³⁺) with exception of **6**[OTf]₃, where the concurring side-reaction with Et₃SiH probably leads to the deactivation of the catalyst.

In conclusion, we have demonstrated that the stabilization of R₂Si²⁺ and RSi³⁺ species with the chelate terpyridine ligand affords stable complex cations, which still behave as Lewis superacids (LSAs), even in the presence of coordinating triflate anions. Theoretical and experimental Lewis acidity scaling corroborates that the terpy-ligated Si-based trications rank with the strongest isolable silicon Lewis acids known to date. The H[–] abstraction from Et₃SiH suggests high hydride

Table 3: Catalytic hydrodefluorination of 1-fluoroadamantane.^[a]

Catalyst	Yield (Et ₃ SiF) [%]	Conv. (C-F) [%]
1 [OTf] ₂	8	23
2 [OTf] ₂	31	48
3 [OTf] ₂	30	51
4 [OTf] ₃	54	> 99
5 [OTf] ₃	56	> 99
6 [OTf] ₃	40	83

[a] Reaction conditions: CH₂CN solutions, 10 mol% catalyst loading, 0.13 M AdF, 2 equiv. of silane. Conversion and yield determined by ¹⁹F NMR integration using fluorobenzene as internal standard after 26 h at room temperature.

ion affinities for **5**³⁺ and **6**³⁺ and represents a promising starting point for E–H bond activation studies beyond Si–H bonds.

Acknowledgements

Funded by the Deutsche Forschungsgemeinschaft (DFG, German Research Foundation) under Germany's Excellence Strategy—EXC 2008–390540038—UniSysCat. A.H. thanks the Einstein Stiftung Berlin for a PhD fellowship. Open access funding enabled and organized by Projekt DEAL.

Conflict of interest

The authors declare no conflict of interest.

Keywords: Coordination compounds · Hydride transfer · Hydrodefluorination · Main group elements · Silanes

- [1] a) O. Sereda, S. Tabassum, R. Wilhelm in *Topics in Current Chemistry* (Ed.: B. List), Springer, Heidelberg, **2009**, pp. 349–393; b) S. A. Weicker, D. W. Stephan, *Bull. Chem. Soc. Jpn.* **2015**, *88*, 1003–1016; c) E. I. Davydova, T. N. Sevastianova, A. Y. Timoshkin, *Coord. Chem. Rev.* **2015**, *297–298*, 91–126; d) D. W. Stephan, G. Erker, *Angew. Chem. Int. Ed.* **2010**, *49*, 46–76; *Angew. Chem.* **2010**, *122*, 50–81.
- [2] T. Stahl, H. F. T. Klare, M. Oestreich, *ACS Catal.* **2013**, *3*, 1578–1587.
- [3] L. Greb, *Chem. Eur. J.* **2018**, *24*, 17881–17896.
- [4] L. O. Müller, D. Himmel, J. Stauffer, G. Steinfeld, J. Slattery, G. Santiso-Quiñones, V. Brecht, I. Krossing, *Angew. Chem. Int. Ed.* **2008**, *47*, 7659–7663; *Angew. Chem.* **2008**, *120*, 7772–7776.
- [5] D. Roth, H. Wadepohl, L. Greb, *Angew. Chem. Int. Ed.* **2020**, DOI: 10.1002/anie.202009736; *Angew. Chem.* **2020**, DOI: 10.1002/ange.202009736.
- [6] a) R. Maskey, M. Schädler, C. Legler, L. Greb, *Angew. Chem. Int. Ed.* **2018**, *57*, 1717–1720; *Angew. Chem.* **2018**, *130*, 1733–1736; b) D. Hartmann, M. Schädler, L. Greb, *Chem. Sci.* **2019**, *10*, 7379–7388.
- [7] H. F. T. Klare, M. Oestreich, *Dalton Trans.* **2010**, *39*, 9176–9184.
- [8] J. C. L. Walker, H. F. T. Klare, M. Oestreich, *Nat. Rev. Chem.* **2020**, *4*, 54–62.
- [9] H. Großekappenberg, M. Reißmann, M. Schmidtman, T. Müller, *Organometallics* **2015**, *34*, 4952–4958.
- [10] M. O'Keeffe, *J. Am. Chem. Soc.* **1986**, *108*, 4341–4343.
- [11] a) W. Koch, G. Frenking, H. Schwarz, F. Maquin, D. Stahl, *J. Chem. Soc. Perkin Trans. 2* **1986**, 757–760; b) J. Roithová, H. Schwarz, D. Schröder, *Chem. Eur. J.* **2009**, *15*, 9995–9999.
- [12] No evidence for the formation of the quasimolecule SiH³⁺ was obtained from collisions of Si³⁺ with H in ion beams. a) C. H. Liu, L. Liu, J. G. Wang, *Phys. Rev. A* **2014**, *90*, 012708; b) H. Bruhns, H. Kreckel, D. W. Savin, D. G. Seely, C. C. Havener, *Phys. Rev. A* **2008**, *77*, 064702.
- [13] a) J. Henker, J. Wirmer-Bartoschek, L. E. Bendel, Y. Xiang, C. Fu, K. Harms, H. Schwalbe, E. Meggers, *Eur. J. Inorg. Chem.* **2016**, 5161–5170; b) D. M. Peloquin, T. A. Schmedake, *Coord. Chem. Rev.* **2016**, *323*, 107–119.
- [14] P. Erdmann, J. Leitner, J. Schwarz, L. Greb, *ChemPhysChem* **2020**, *21*, 987–994.
- [15] K. Müther, P. Hrobárik, V. Hrobáriková, M. Kaupp, M. Oestreich, *Chem. Eur. J.* **2013**, *19*, 16579–16594.

- [16] a) V. Barone, M. Cossi, *J. Phys. Chem. A* **1998**, *102*, 1995–2001; b) M. Cossi, N. Rega, G. Scalmani, V. Barone, *J. Comput. Chem.* **2003**, *24*, 669–681.
- [17] I. Krossing, A. Bihlmeier, I. Raabe, N. Trapp, *Angew. Chem. Int. Ed.* **2003**, *42*, 1531–1534; *Angew. Chem.* **2003**, *115*, 1569–1572.
- [18] S. S. Chitnis, F. Krischer, D. W. Stephan, *Chem. Eur. J.* **2018**, *24*, 6543–6546.
- [19] R. Damrauer, R. A. Simon, B. Kanner, *Organometallics* **1988**, *7*, 1161–1164.
- [20] G. Meier, T. Braun, *Angew. Chem. Int. Ed.* **2009**, *48*, 1546–1548; *Angew. Chem.* **2009**, *121*, 1575–1577.
- [21] S. E. Johnson, R. O. Day, R. R. Holmes, *Inorg. Chem.* **1989**, *28*, 3182–3189.
- [22] A. Del Grosso, R. G. Pritchard, C. A. Muryn, M. J. Ingleson, *Organometallics* **2010**, *29*, 241–249.
- [23] a) U. Mayer, V. Gutmann, W. Gerger, *Monatsh. Chem.* **1975**, *106*, 1235–1257; b) M. A. Beckett, G. C. Strickland, J. R. Holland, K. Sukumar Varma, *Polymer* **1996**, *37*, 4629–4631.
- [24] J. J. Jennings, B. W. Wigman, B. M. Armstrong, A. K. Franz, *J. Org. Chem.* **2019**, *84*, 15845–15853.
- [25] a) E. L. Myers, C. P. Butts, V. K. Aggarwal, *Chem. Commun.* **2006**, 4434–4436; b) A. R. Nödling, K. Mütther, V. H. G. Rohde, G. Hilt, M. Oestreich, *Organometallics* **2014**, *33*, 302–308.
- [26] a) R. J. Blagg, T. R. Simmons, G. R. Hatton, J. M. Courtney, E. L. Bennett, E. J. Lawrence, G. G. Wildgoose, *Dalton Trans.* **2016**, *45*, 6032–6043; b) A. E. Ashley, T. J. Herrington, G. G. Wildgoose, H. Zaher, A. L. Thompson, N. H. Rees, T. Krämer, D. O'Hare, *J. Am. Chem. Soc.* **2011**, *133*, 14727–14740.
- [27] G. A. Olah, K. Laali, O. Farooq, *Organometallics* **1984**, *3*, 1337–1340.
- [28] J. E. Radcliffe, J. J. Dunsford, J. Cid, V. Fasano, M. J. Ingleson, *Organometallics* **2017**, *36*, 4952–4960.
- [29] A. E. Waked, S. S. Chitnis, D. W. Stephan, *Chem. Commun.* **2019**, *55*, 8971–8974.
- [30] a) S. Bähr, M. Oestreich, *Chem. Eur. J.* **2018**, *24*, 5613–5622; b) C. D. F. Königs, H. F. T. Klare, M. Oestreich, *Angew. Chem. Int. Ed.* **2013**, *52*, 10076–10079; *Angew. Chem.* **2013**, *125*, 10260–10263; c) D. V. Gutsulyak, A. van der Est, G. I. Nikonov, *Angew. Chem. Int. Ed.* **2011**, *50*, 1384–1387; *Angew. Chem.* **2011**, *123*, 1420–1423.
- [31] Deposition numbers 2023615, 2023616, 2023617, 2023618, 2023619, 2023620, 2023625 and 2023626 (triflate salts of 1^{2+} , 3^{2+} , 2^{2+} , $[2(F)]^+$, 4^{3+} , 6^{3+} , $[6(OPEt_3)]^{3+}$ and $[5(H)]^{2+}$) contain the supplementary crystallographic data for this paper. These data are provided free of charge by the joint Cambridge Crystallographic Data Centre and Fachinformationszentrum Karlsruhe Access Structures service.

Manuscript received: August 26, 2020

Accepted manuscript online: September 16, 2020

Version of record online: October 15, 2020